Simple acyclic molecules containing a single charge-assisted O–H group can recognize anions in acetonitrile:water mixtures

Rosemary J. Goodwin, Mitchell T. Blyth, Alfred K. K. Fung, Leesa M. Smith, Philip L. Norcott, Sara Tanovic, Michelle L. Coote* and Nicholas G. White*

Hydroxypyridinium and hydroxyquinolinium compounds containing acidic O–H groups attached to a cationic aromatic scaffold were synthesized, *i.e. N*-methyl-3-hydroxypyridinium (**1**$^+$) and *N*-methyl-8-hydroxyquinolinium (**2**$^+$). These very simple compounds are capable of binding to chloride very strongly in CD_3CN and with moderate strength in 9:1 CD_3CN:D_2O. Comparison with known association constants reveal that **1**$^+$ and **2**$^+$ bind chloride in CD_3CN or CD_3CN:D_2O with comparable affinities to receptors containing significantly more hydrogen bond donors and/or higher positive charges. Crystal structures of both compounds with coordinating anions were obtained, and feature short O–H···anion hydrogen bonds. A receptor containing two hydroxyquinolinium groups was also prepared. While the low solubility of this compound caused difficulties, we were able demonstrate chloride binding in a competitive 1:1 CD_3CN:CD_3OD solvent mixture. Addition of sulfate to this compound results in the formation of a crystallographically-characterised solid state anion coordination polymer.

Introduction

The development of anion recognition and its application in a range of fields has been an ongoing research target within supramolecular chemistry.[1,2] Many of the initial receptors bound anions through N–H···anion interaction, although more recently C–H···anion hydrogen bonding,[3] as well as halogen bonding[4] and other sigma-hole interactions[5] have been developed as recognition motifs. While O–H···anion interactions have been studied intermittently for several decades, they have received relatively little attention, particularly given their potential ease of synthesis and strong hydrogen bond character.[6]

Early studies revealed that simple O–H-containing molecules such as sugars, catechol and alizarin can bind anions in polar organic solvents.[7-9] More recently, it has been demonstrated that incorporating O–H hydrogen bond donors into more complex scaffolds such as foldamers[10,11] or metal organic frameworks[12] can achieve impressive guest recognition, while using O–H hydrogen bonds in conjunction with a Lewis acidic boron centre can give selective fluoride binding in THF:water mixtures.[13] As the field of anion supramolecular chemistry has expanded beyond simple anion recognition to applications,[14,15] so O–H··anion interactions have been used in a range of applications including self–assembly,[16,17] anion transport,[18-20] and organocatalysis.[21-23]

It would appear that the development of strong O–H···anion binding motifs would facilitate further applications in these fields. Given that even relatively simple neutral O–H containing molecules can be surprisingly potent anion receptors,[8,9,24,25] it is likely that cationic hosts containing strong O–H hydrogen bond donors may be able to achieve high anion affinities in competitive solvent media, although very few such receptors have been prepared. Alfonso has reported di- and tricationic O–H containing receptors that can function in acetonitrile/methanol mixtures,[26] while we have recently reported simple cationic acyclic receptors containing amide and phenol hydrogen bond donors that can function in 9:1 acetonitrile:water.[27] In the current work, we describe the anion recognition properties of a family of simple cationic molecules that contain very strong O–H hydrogen bond donors (Figure 1). These molecules can be prepared in one step from commercially-available and cheap 3-hydroxypridine or 8-hydroxyquinoline. While they are prone to deprotonation by basic anions, we show that they are able to bind anions in acetonitrile:water mixtures.

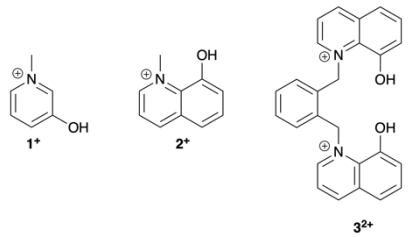

Figure 1 Cationic molecules containing strong O–H hydrogen bond donors used in this work.

Results

Synthesis

Synthesis of 1$^+$, 2$^+$ and 3^{2+}: Compounds **1**$^+$ and **2**$^+$ were prepared as their iodide salts by alkylation of commercially-available 3-hydroxypyridine or 8-hydroxyquinoline using methyl iodide.[28,29] Alkylation of **1**$^+$ proceeds quantitatively, while a side-product is produced during the alkylation of **2**$^+$. However, this is not troublesome as **2·I** precipitates from the acetonitrile reaction solution (see Supporting Information for an optimized preparation of **2·I** on a multi-gram scale).

Research School of Chemistry, Australian National University, Canberra, ACT, Australia.
Email: michelle.coote@anu.edu.au, nicholas.white@anu.edu.au
Website: rsc.anu.edu.au/~mcoote/, www.nwhitegroup.com
† Electronic Supplementary Information (ESI) available: additional synthetic details, characterization data, details of anion binding, X-ray crystallography, pK_a measurements and computational studies.

The bis-hydroxyquinolinium compound $\mathbf{3}^{2+}$ was synthesized from commercially available 8-hydroxyquinoline and 1,2-bis(bromomethyl)benzene (Scheme 1). The reaction of ten equivalents of hydroxyquinoline with bis(bromomethyl)benzene in refluxing acetonitrile gave a yellow precipitate in approximately 55% yield, which ^{1}H NMR spectroscopy showed was $\mathbf{3{\cdot}Br_2}$ of ~ 90% purity (see Supporting Information for more details). Purification by column chromatography eluting with a basic DCM/MeOH/NEt_3 mixture and then precipitating using $HBr_{(aq)}$ gave pure $\mathbf{3{\cdot}Br_2}$. It appears that several side-products form during the reaction resulting from *O*-alkylation reactions: one of these, **4·Br** could be isolated from the reaction mixture and was characterized crystallographically and by NMR spectroscopy (Scheme 1, and ESI). A "tidier" synthesis of $\mathbf{3{\cdot}Br_2}$ may well be possible starting from 8-methoxyquinoline and bis(bromomethyl)benzene followed by demethylation, however given that the starting materials used in our synthesis are cheap, and purification relatively simple, this was not investigated.

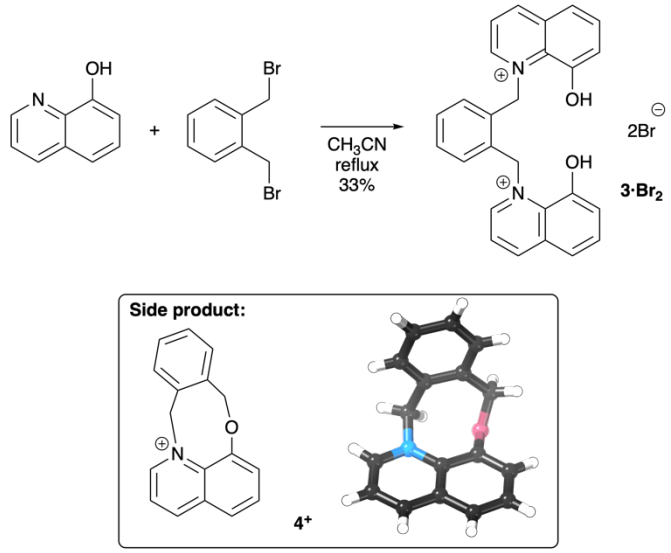

Scheme 1 Synthesis of $\mathbf{3{\cdot}Br_2}$, structure of side product **4·Br**, and X-ray crystal structure of cation $\mathbf{4}^+$.

Anion exchange: We exchanged the potentially coordinating halide anions in **1·I**, **2·I** and $\mathbf{3{\cdot}Br_2}$ for non-coordinating hexafluorophosphate or tetraphenylborate anions by precipitation in good yields (86–93%). We prepared the hexafluorophosphate salt of $\mathbf{3}^{2+}$ and found that it was best to add a few drops of 1% $HPF_{6(aq)}$ to avoid the products having an orange colour, which we attribute to traces of deprotonated species (see later).

In the case of $\mathbf{1}^+$, we could not isolate the PF_6^- salt as this did not precipitate from water. In the case of $\mathbf{2}^+$, it was possible to isolate a crystalline solid when a concentrated aqueous solution of hot **2·I** was mixed with aqueous NH_4PF_6 and allowed to cool. SCXRD studies of one of these crystals showed that it was $\mathbf{2{\cdot}PF_6}$, and ^{1}H and ^{13}C NMR analyses of the bulk material were satisfactory. However, quantitative ^{19}F NMR spectroscopy[30] revealed a lower amount of PF_6^- than expected (approximately one half) suggesting that anion exchange was incomplete and the material was a mixture of the I^- and PF_6^- salt. Mixing a solution of this material in acetone with $AgBF_4$ in acetone resulted in the formation of cloudy precipitate (presumably AgI), supporting this hypothesis.

Given that we could not satisfactorily isolate PF_6^- salts of $\mathbf{1}^+$ or $\mathbf{2}^+$, these compounds were instead isolated as the tetraphenylborate salts by precipitation from methanol. Integration of the ^{1}H NMR spectrum confirmed that complete anion exchange had been achieved in these cases, and integration of the quantitative ^{19}F NMR spectrum[31] of $\mathbf{3{\cdot}(PF_6)_2}$ indicated complete conversion to the hexafluorophosphate salt.

Deprotonation: We initially attempted to convert $\mathbf{2}^+$ and $\mathbf{3}^{2+}$ to their PF_6^- salts using a relatively old bottle of NH_4PF_6. This resulted in deep orange-coloured solutions or precipitates; an intense orange-red colour is known to result from deprotonated hydroxyquinolinium groups, which display significant solvatochromic effects.[28] Analysis of this bottle of NH_4PF_6 using ^{19}F NMR spectroscopy revealed that it contained a significant amount of F^-, which presumably acted as a base to partially deprotonate the compounds resulting in the deeply-coloured zwitterionic form. Adding small amounts of triethylamine to solutions of the compounds produced similar colours, and we were able to obtain single crystals of $\mathbf{3^{-H}{\cdot}PF_6}$ suitable for X-ray diffraction studies in this way. X-ray crystallography reveals a very short O–H···O$^-$ distance, with a distance of 2.414(2) Å between the two oxygen atoms.[31] This hydrogen bond links the structure into a one-dimensional hydrogen bonded chain (Figure 2).

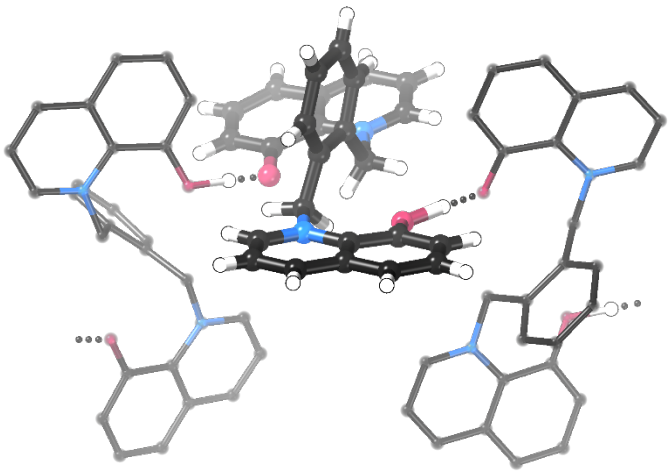

Figure 2 X-ray crystal structure of $\mathbf{3^{-H}{\cdot}PF_6}$ (PF_6^- anions and some C–H hydrogen atoms are omitted for clarity). Note: PLATON-SQUEEZE was used.[32]

To investigate this further, we attempted to measure the pK_a of $\mathbf{3{\cdot}Br_2}$ in water to allow comparison with that of $\mathbf{2}^+$, which is 6.8.[33] Unfortunately precipitation meant we were unable to do so quantitatively, but qualitatively, the pK_a of $\mathbf{3}^{2+}$ appears to be broadly similar to that of $\mathbf{2}^+$, suggesting the acidity of each O–H group is relatively independent of the other.[34] Due to the low

solubility of $\mathbf{3^{-H}{\cdot}PF_6}$ in polar solvents, it was possible to isolate it as a crystalline solid by adding one equivalent of triethylamine to a methanol solution of $\mathbf{3{\cdot}(PF_6)_2}$ (Scheme 2). NMR spectroscopy, including integration of the ^{1}H NMR and quantitative ^{19}F NMR spectrum[31] against a standard confirmed that $\mathbf{3^{-H}{\cdot}PF_6}$ was isolated selectively.

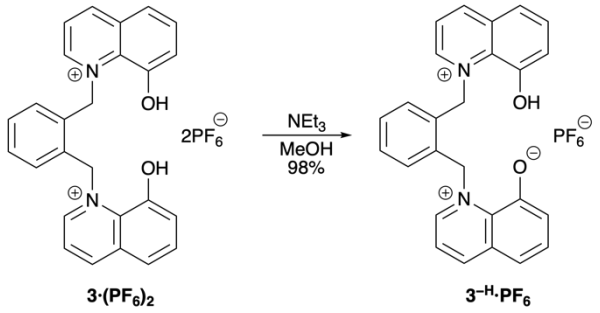

Scheme 2 Synthesis of $\mathbf{3^{-H}{\cdot}PF_6}$.

Anion binding of $\mathbf{1^+}$ and $\mathbf{2^+}$

NMR titrations: A preliminary qualitative screen of anion binding was conducted by adding one equivalent of anion to 1.0 mM solutions $\mathbf{2^+}$ in either CH_3CN or 9:1 CH_3CN:H_2O. This revealed that $H_2PO_4^-$ caused precipitation, while OAc^- caused deprotonation in both solvent systems and so these anions were not studied quantitatively (Figures S25 and S26). Instead we focused on Cl^- and SO_4^{2-} and studied guest binding using quantitative ^{1}H NMR titration experiments. Addition of chloride anion to either $\mathbf{1^+}$ or $\mathbf{2^+}$ in CD_3CN resulted in significant downfield shifts of hydrogen atoms adjacent to the O–H group (Figure 3, Figures S29–S34).[35] Fitting the peak movement to a 1:1 binding isotherm using *Bindfit*,[36] revealed that association of chloride with both of these receptors was too high to be determined by NMR titration experiments (> 10^4 M^{-1}). Addition of sulfate resulted in precipitation.

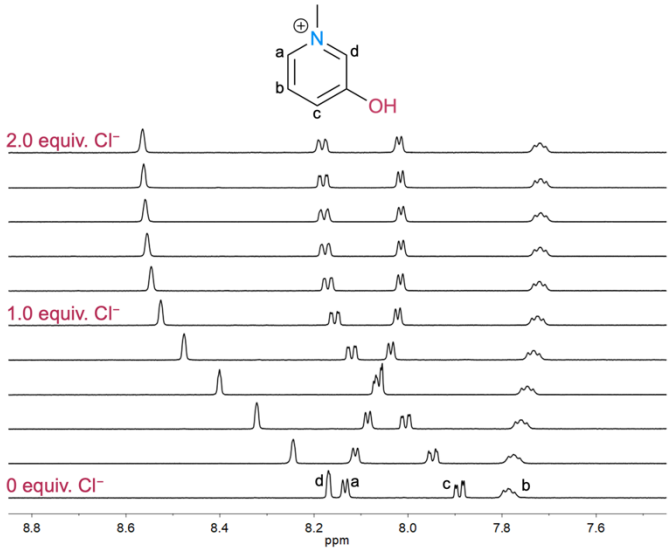

Figure 3 Partial ^{1}H NMR spectra of $\mathbf{1{\cdot}BPh_4}$ upon addition of TBA·Cl (CD_3CN, 600 MHz, 298 K). The 11 spectra represent 0–2.0 equivalents of Cl^- at intervals of 0.2 equivalents.

Given the very strong binding in CD_3CN, we next studied binding in the highly competitive mixed organic/aqueous system 9:1 CD_3CN:D_2O. Interestingly, chloride caused small downfield shifts in C–H protons adjacent to the O–H group, while sulfate caused upfield shifts. We do not know the reason for this, although it does not appear to be due to deprotonation.[37] In this competitive solvent mixture, binding was significantly weaker than in pure acetonitrile, but moderate binding was still observed by $\mathbf{1^+}$, with very weak binding observed by $\mathbf{2^+}$ (Table 1). The stronger binding observed for $\mathbf{1^+}$ compared to $\mathbf{2^+}$ is not unexpected as $\mathbf{1^+}$ is known to have a more acidic O–H group than $\mathbf{2^+}$ (the pK_a values in water are 5.0 [38] and 6.8,[33] respectively).

Table 1. Association constants (M^{-1}) for $\mathbf{1{\cdot}BPh_4}$ and $\mathbf{2{\cdot}BPh_4}$ with anions.[a]

Receptor, solvent	Cl^-	SO_4^{2-}
$\mathbf{1{\cdot}BPh_4}$, CD_3CN	> 10^4	precipitation
$\mathbf{2{\cdot}BPh_4}$, CD_3CN	> 10^4	precipitation
$\mathbf{1{\cdot}BPh_4}$, 9:1 CD_3CN:D_2O	65(3)	77(8)
$\mathbf{2{\cdot}BPh_4}$, 9:1 CD_3CN:D_2O	13(1)	negligible

[a] Anions added as TBA salts, 1:1 binding constants calculated using *Bindfit*,[36] the asymptotic error[39] is provided at the 95% confidence interval in parentheses.

X-ray crystal structures: We were able to obtain several crystal structures of $\mathbf{1^+}$ and $\mathbf{2^+}$ with various anions: the structures of $\mathbf{1{\cdot}I}$, $\mathbf{2{\cdot}Cl}$ and $\mathbf{2_2{\cdot}SO_4}$ are presented in Figure 4, while additional structures ($\mathbf{1{\cdot}BPh_4}$, $\mathbf{2{\cdot}PF_6}$) are discussed in the Supporting Information. As shown, H···anion distances are short ranging from as little as 64% of the sum of the van der Waals radii[40] (Σ_{vdW}) in the structure of $\mathbf{2_2{\cdot}SO_4}$ to 71% of Σ_{vdW} in $\mathbf{2{\cdot}Cl}$, to 76–80% of Σ_{vdW} in $\mathbf{2{\cdot}I}$. In the structures of $\mathbf{1{\cdot}BPh_4}$ and $\mathbf{2{\cdot}PF_6}$, no O–H···anion interactions shorter than Σ_{vdW} are observed, consistent with the non-coordinating nature of these anions. We note that the 71% of Σ_{vdW} in $\mathbf{2{\cdot}Cl}$ is similar to the 72% Σ_{vdW} observed in the previously-reported structure of $\mathbf{1{\cdot}Cl}$.[41,42]

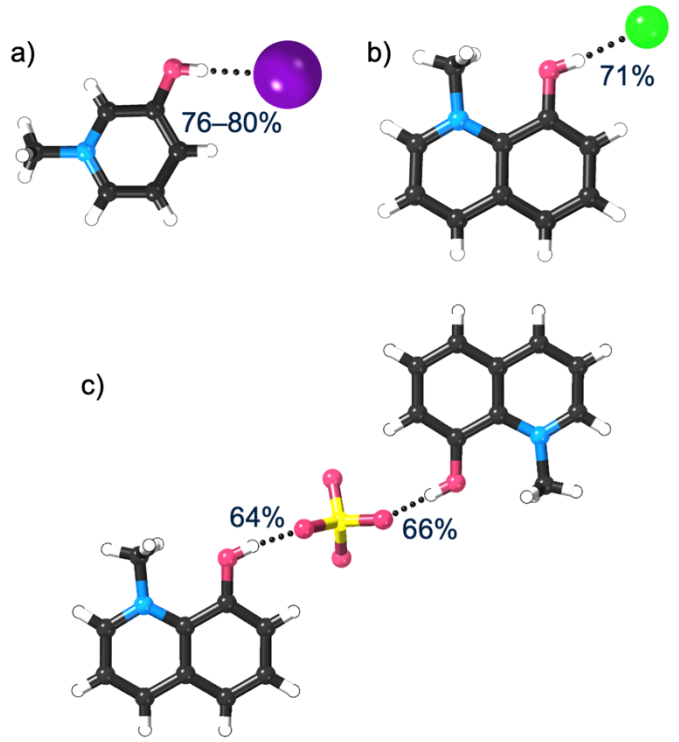

Figure 4 X-ray crystal structures of a) **1·I**, b) **2·Cl**, and c) **2_2·SO_4**. H···acceptor distances for hydrogen bonds are given as Σ_{vdW}.[40] A range is given for **1·I** as this structure has Z' = 5 so there are several different H···I^- distances. Positional disorder of the anion in **2_2·SO_4** is omitted for clarity.

Anion binding of 3^{2+}

NMR titrations: 3·$(PF_6)_2$ suffers from poor solubility, and is not appreciably soluble in a range of polar organic solvents, including acetonitrile and acetonitrile/water mixtures. We were therefore not able to conduct binding studies in the same solvent mixture used for 1^+ and 2^+. Instead, anion recognition was studied using ^{1}H NMR titration experiments in competitive 1:1 CD_3CN:CD_3OD. As was the case for 1^+ and 2^+, a preliminary screen (Figure S23) revealed that $H_2PO_4^-$ caused precipitation, while OAc^- caused deprotonation and so these anions were not studied quantitatively.

Addition of chloride to 3^{2+} resulted in small but significant downfield shifts in the C–H proton resonances close to the hydroxy groups and the peak movement was fitted to a 1:1 binding isotherm using *Bindfit*.[36] This revealed that chloride bound with moderate strength in this polar solvent mixture [K_a = 76(2) M^{-1}]. Addition of sulfate to 3^{2+} caused precipitation and so we were unable to calculate an association constant.

X-ray crystal structures: We were able to obtain several crystal structures of 3^{2+}, which are shown in Figure 5. Interestingly, when there are no coordinating anions available in the structure of **3·$(PF_6)_2$** the receptor adopts an *anti* configuration where the two O–H groups point in opposite directions and form short hydrogen bonds (66, 71% Σ_{vdW}[40]) to acetonitrile solvent molecules. Another structure of **3·$(PF_6)_2$** was obtained from a different solvent mixture and has a similar structure (see Supporting Information). In the structure of **3·Br_2**, an *anti* configuration of the cation is also observed, presumably to facilitate hydrogen bonding to each anion. When **3·$(PF_6)_2$** was crystallised in the presence of one equivalent of either Cl^- or Br^-, crystals of **3·Cl·PF_6** and **3·Br·PF_6** were obtained (Figure 5c and 5d). In these structures, the receptor adopts a *syn* configuration with both O–H groups forming relatively short hydrogen bonds to the halide anion. Hydrogen bonds are slightly shorter as Σ_{vdW} with chloride than with bromide. Very small crystals of **3·SO_4** were obtained, which required the use of synchrotron radiation.[43] In this case, the molecule adopts an *anti* configuration and short hydrogen bonds between 3^{2+} and sulfate (64, 65% Σ_{vdW}) result in the formation of a one-dimensional hydrogen bonded polymer assembled by anion coordination.[44-46] Two methanol solvent molecules also hydrogen bond to the sulfate anion, although these hydrogen bonds are longer (70, 74% Σ_{vdW}).

Colourimetric "anion" sensing by 2^+, 3^{2+} and 3^{-H+}

As noted above, pale yellow solutions of **2·BPh_4** take on a deep orange-red colour in the presence of OAc^- (Figures S25 and S26), which we attribute to deprotonation of 2^+ to form the zwitterionic form, which is a known chromophore.[28] A similar phenomenon is observed when OAc^- is added to 3^{2+} (Figure S27). Additionally, red solutions of **3^{-H+}·PF_6** partially decolourise upon addition of HSO_4^- (Figure S28), which we attribute to partial protonation of 3^{-H+} by the acidic HSO_4^- anion (pK_a = 2.0).[47] While these colourimetric responses suggest an anion sensing response (and similar responses are sometimes reported in the literature as such[6]), this is not really an accurate description of what is occurring, and the compounds are instead simply responding to base/acid.

pK_a measurements of 2^+

We investigated the effect of solvent and anion on the p*K*a values of these highly acidic O–H groups. Unfortunately, the low solubility of 3^{2+} prohibited the determination of quantitative pK_a measurements and so we focused attention on 2^+.

Solvent effects: We conducted measurements in 9:1 MeOH:H_2O and DMF to complement the known value in H_2O.[33] Unsurprisingly, moving towards less polar solvents increases the pK_a of 2^+, with this value increasing from 6.8 in water, to 7.5 in MeOH:H_2O and 9.5 in DMF (Table 2).

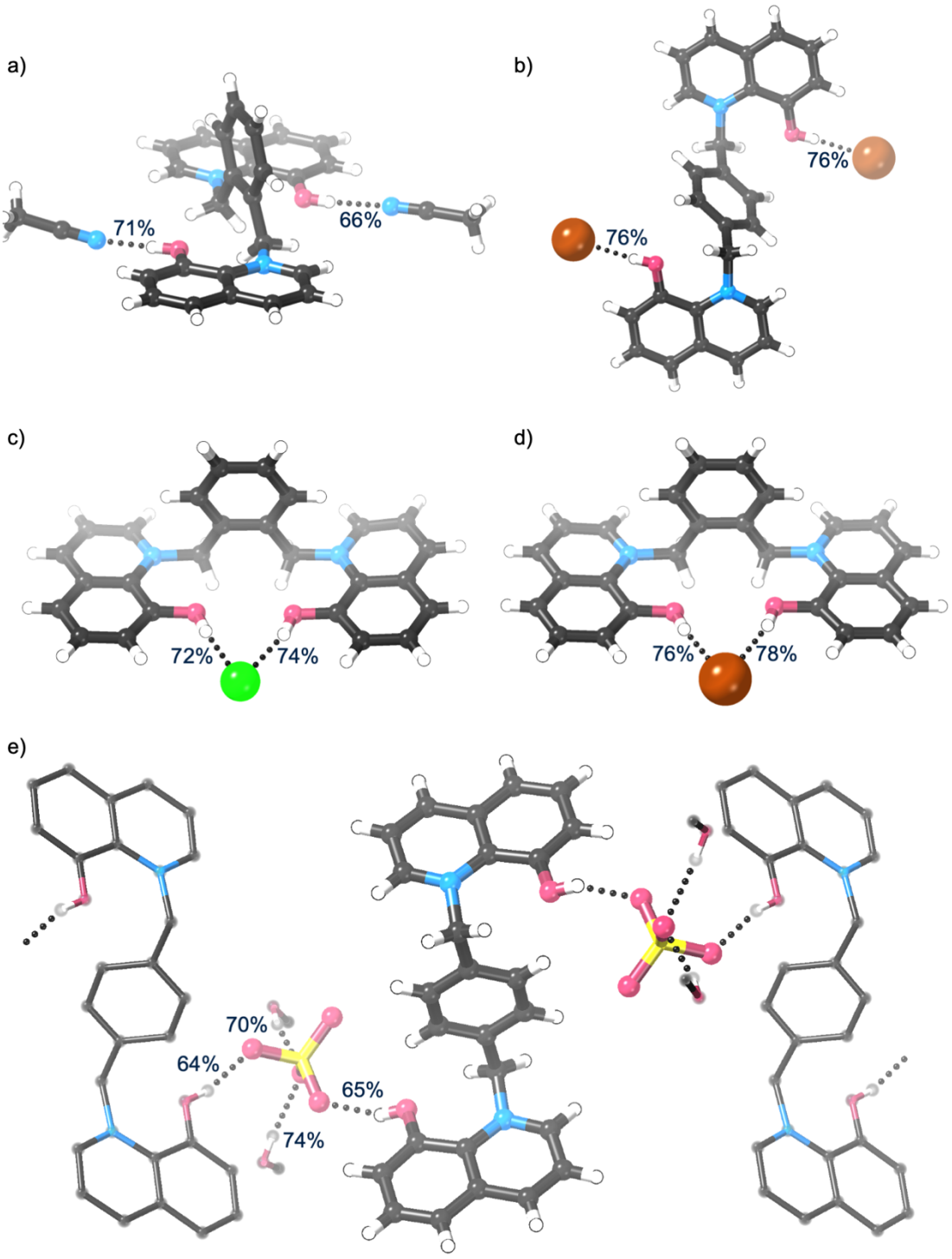

Figure 5 X-ray crystal structures of a) **3·(PF$_6$)$_2$**, b) **3·Br$_2$**, c) **3·Cl·PF$_6$**, d) **3·Br·PF$_6$** and e) **3·SO$_4$**. H···acceptor distances for hydrogen bonds are given as Σ_{vdW}.[40] The structure of **3·(PF$_6$)$_2$** has Z′=2, only part of the unit cell is shown for clarity. Most solvent molecules and the PF_6^- anions are omitted for clarity.

Anion effects: We were interested to see whether the anion present affected the pK_a of the O–H group in **2**$^+$. To investigate this we prepared **2·Cl** in good yield by precipitation from acetone (see Experimental Section). We reasoned that a favourable O–H···Cl$^-$ hydrogen bond might favour the protonated form of **2**$^+$ and thus increase the pK_a of **2·Cl** relative to **2·BPh$_4$**,[48] which cannot form a strong hydrogen bond, and so measured the pK_as of these compounds in both 9:1 MeOH:H_2O and DMF. Unsurprisingly, in 9:1 MeOH:H_2O, no difference in pK_a is observed between **2·Cl** and **2·BPh$_4$**, which we attribute to negligible hydrogen bonding between **2**$^+$ and Cl$^-$ in this very competitive solvent mixture. We were also not able to obtain evidence of a difference in pK_as between **2·Cl** and **2·BPh$_4$** in

DMF, which is perhaps somewhat surprising. More details of these experiments and the rationale behind them are provided in the ESI.

Table 2. pK_a values of **2·Cl** and **2·BPh$_4$** in different solvents, with the estimated 95% confidence interval of the mean.[a]

Solvent	pK_a for 2·Cl	pK_a for 2·BPh$_4$
H_2O	6.8 [33]	–
9:1 MeOH:H_2O[b]	7.4 ± 0.1	7.5 ± 0.1
DMF[c]	9.5 ± 0.2	9.5 ± 0.1

[a] ± 2 standard errors (SE) of the mean, which were estimated as SE = $\sigma/\sqrt{n}$. [b]Determined by potentiometric titrations using NaOH as base. [c]Determined by potentiometric titrations using DBU as base.

Computational studies and discussion

Compounds **1**$^+$ and **2**$^+$ each appear to have only one significant hydrogen bond donor, *i.e.* the O–H group. In the crystal structures, these groups are the only ones that form short hydrogen bonds, although contacts slightly shorter than the sum of the vdW radii also observed on some occasions between the anion and the C–H group adjacent to the O–H group.[49] To investigate the energetic contributions of these possible interactions, we conducted density functional theory calculations at the M06-2X/6-311+G(d,p) level of theory.[50] We minimised the structures of **1·Cl** and **2·Cl** using an SMD continuum solvent model[51] to account for solvent effects, and then used Natural Bond Orbital (NBO) analysis to calculate the relative contributions of the possible interactions (see the ESI for full details). These calculations reveal that 88–90% of the binding energy is accounted for by O–H···Cl$^-$ interactions, *i.e.* that other contributions are minimal and this single hydrogen bond is responsible for the vast majority of the binding (Tables S13–S15).

Despite the fact that **1**$^+$ and **2**$^+$ each contain only one significant hydrogen bond donor, they are able to bind anions strongly, with association constants for chloride > 10^4 M^{-1} in acetonitrile, and respectable values obtained in competitive 9:1 acetonitrile:water mixtures. To put this in context, we have compared these association constants with known receptors that have been reported to bind Cl$^-$ in acetonitrile or 9:1 acetonitrile:water. Unsurprisingly, **1**$^+$ and **2**$^+$ bind chloride more strongly than neutral molecules containing a single O–H group. Interestingly, this is true even for molecules with similarly acidic O–H groups, suggesting that electrostatic attraction is important as well as the acidity of the O–H hydrogen bond. For example, 4-nitrophenol has a very similar pK_a to **2**$^+$ (7.1 [52] compared with 6.8 [33] for **2**$^+$), but binds chloride with an association constant of only 560 M^{-1} in CD_3CN.[53] It is notable that **1**$^+$ and **2**$^+$ also bind chloride more strongly than similarly acidic molecules containing more O–H donors: for example, 4-nitrocatechol which has two highly acidic O–H groups (pk_a = 6.7 [54], K_a = 4,400 M^{-1} for Cl$^-$ in CD_3CN).[9]

While the electrostatic attraction for anions in **1**$^+$ and **2**$^+$ is presumably important, it is clearly not the only factor. For example, **1**$^+$ displays similar chloride binding affinities in 9:1 CD_3CN:D_2O to charged receptors containing a pyridinium group and two phenolic O–H and two amide groups (65 M^{-1} for **1**$^+$ *vs.* 61–170 M^{-1}).[27,55] Indeed, the association constant between **1**$^+$ and Cl$^-$ in 9:1 CD_3CN:D_2O (65 M^{-1}) is within one order of magnitude of those reported for a di-cationic bis-imidazolium macrocycle **4**$^{2+}$ (structure provided in Figure 6, K_a 163 M^{-1}),[56] tetra-cationic tetra-imidazolium macrocycles[57] and tetra-imidazolium catenanes (binding constants and structures for these compounds are provided in Figure S69).[56]

To investigate the effects of the various contributions to guest binding, we used Energy Decomposition Analysis based on Absolutely Localised Molecular Orbitals within a continuum solvent model [ALMO-EDA(solv)],[58] to tease apart the respective contributions to binding energies. It should be noted that these calculations isolate the contributions to the solution phase electronic energy and do not consider entropy, which would be expected to have a relatively consistent contribution as the same anion and solvent are being compared in all cases. The calculations suggest that in acetonitrile binding of chloride to any of **1**$^+$, **2**$^+$ or the macrocycle **4**$^{2+}$ is significantly stronger than binding to nitrocatechol, which is itself significantly stronger than chloride binding to nitrophenol (as expected based on measured association constants). In 9:1 MeCN:H_2O, binding of chloride to macrocycle **4**$^{2+}$ is more favourable than binding to **1**$^+$, but not by a huge amount.

As would be expected and as shown graphically in Figure 6, dicationic **4**$^{2+}$ has a significantly more favourable electrostatic component (–758 kJ mol^{-1}) than mono-cationic **1**$^+$ and **2**$^+$ (–471 – –477 kJ mol^{-1}) or neutral nitrocatechol and nitrophenol (–214 – –316 kJ mol^{-1}). This favourability is largely counteracted however, by a significantly higher solvation penalty for **4**$^{2+}$ (636 kJ mol^{-1} for **4**$^{2+}$, 329 – 330 kJ mol^{-1} for **1**$^+$ and **2**$^+$, 95 – 123 kJ mol^{-1} for the neutral molecules). A more detailed data breakdown, including a similar analysis for **1**$^+$ and **4**$^{2+}$ in 9:1 CH_3CN:H_2O is provided in the ESI.

Clearly recognition of chloride by more complex anion receptors is complicated by preorganisation effects, *i.e.* it is non-trivial to design a receptor where all donors can interact with the anion without significant reorganisation. Nevertheless, it is remarkable that **1**$^+$ and **2**$^+$ can effect chloride recognition in aqueous acetonitrile using a single charge-assisted O–H group, and that the strength of this is broadly comparable to receptors with a much higher charge and/or far more hydrogen bond donors. Calculations suggest that the combination of electrostatic attraction for the anion, coupled with an acidic hydrogen bond donor, and a relatively low solvation energy penalty drive the favourable binding of chloride to **1**$^+$ and **2**$^+$. Taken together, our results suggest that receptors with few binding sites may bind guests more strongly than would otherwise be expected, due to their lower solvation penalties.

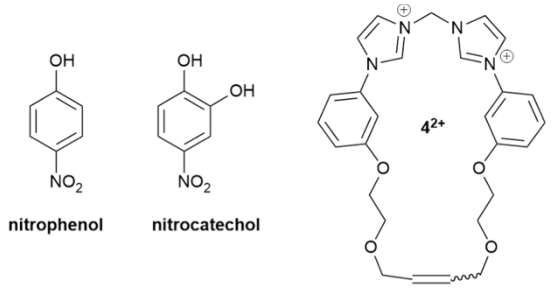

Compound	pK_a	K_a Cl^- (M^{-1}) CD_3CN	K_a Cl^- (M^{-1}) 9:1 CD_3CN:D_2O
Nitrophenol	7.1 [53]	560 [54]	–
Nitrocatechol	6.7 [55]	4,400 [9]	–
1$^+$	5.0 [39]	> 10^4	65
2$^+$	6.8 [34]	> 10^4	13
4^{2+}	–	–	163 [56]

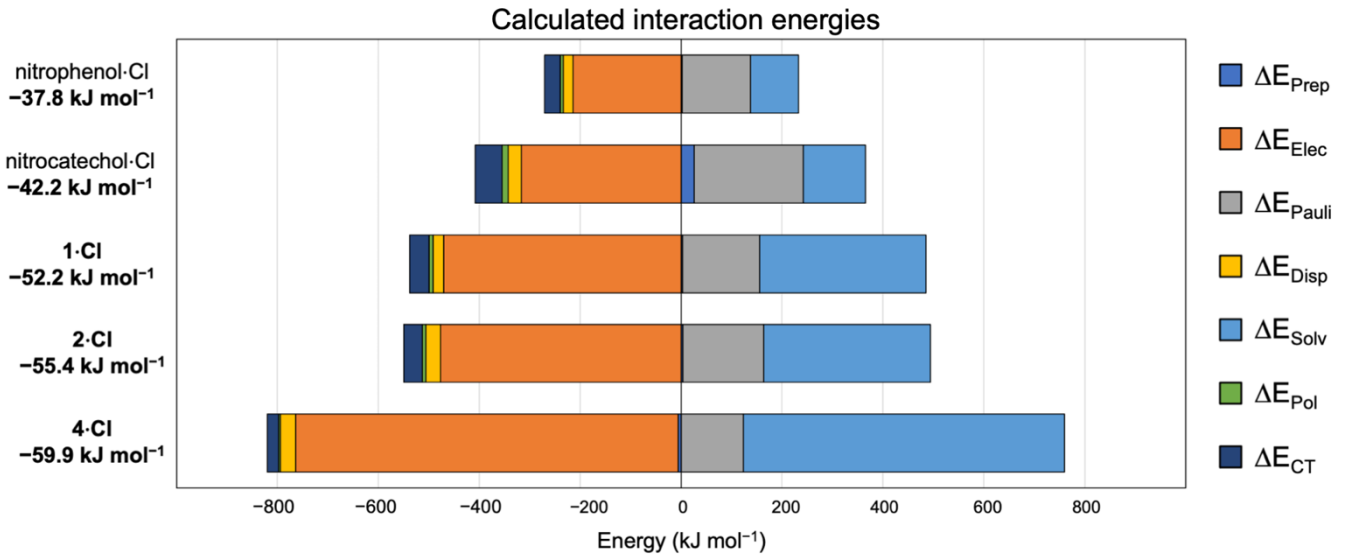

Figure 6 Structures of molecules investigated computationally, their association constants for chloride, and ALMO-EDA(solv.) contributions to calculated interaction energies. The overall interaction energies are given to the left of the chart. ΔE_{Prep} is preparation energy, ΔE_{Elec} is the electrostatic component, ΔE_{Pauli} is the Pauli repulsion energy, Δ_{Disp} is the dispersion energy, ΔE_{Solv} is the solvation energy contribution, ΔE_{Pol} is the polarisation contribution and ΔE_{CT} is the charge transfer energy.

Conclusions

We have investigated the anion recognition capability of the simple molecules **1**$^+$ and **2**$^+$, which contain a single strong O–H hydrogen bond donor. These molecules display strong chloride binding in CD_3CN (K_a > 10^4 M^{-1}), and moderate chloride binding in 9:1 CD_3CN:D_2O (K_a = 65 and 13 M^{-1}, respectively). These association constants are much higher than neutral compounds containing similarly acidic O–H groups, and are comparable to highly charged receptors. Computational studies suggest this is due to a favourable balance of electrostatic attraction with a relatively low degree of solvation.

While it is clear that these types of molecules are prone to deprotonation, it seems likely that hosts incorporating two or more hydroxypyridinium or hydroxyquinolinium groups would be very potent anion receptors. Unfortunately our first attempts to investigate such systems in the form of **3**$^{2+}$ were hampered by this compound's low solubility. This compound is also apparently poorly preorganised such that **3**$^{2+}$ has to rearrange from an *anti* to *syn* conformation to bind anions. Nevertheless, we suggest that future receptors containing well-designed charged O–H groups would be worthy targets of further investigation.

Experimental

Characterisation data, details of instrumentation, anion binding experiments, pK_a measurements, X-ray crystallography and computational studies are provided in the ESI.

General remarks

The reaction of 3-hydroxypyridine and methyl iodide in *n*-propanol afforded **1·I** quantitatively, as previously reported.[29,59] **2·I** was prepared on a multi-gram scale by a slight modification of a previously reported procedure[28] (see ESI). The synthesis of $DBU^H{\cdot}PF_6$ from DBU is described in the ESI.

1·BPh_4: A solution of **1·I** (0.237 g, 1.00 mmol) in MeOH (10 mL) was added to a solution of $NaBPh_4$ (0.411 g, 1.20 mmol) in MeOH (10 mL) resulting in the immediate formation of a white precipitate. The suspension was allowed to stand for 30 minutes, and then filtered. The resulting white microcrystalline solid was washed with MeOH (3 × 5 mL) and then thoroughly

air-dried to give **1·BPh$_4$**. Yield: 0.367 g (0.856 mmol, 86%).

^{1}H NMR (CD_3CN): 8.15 (br. s, 1H), 8.10 (d, *J* = 7.8 Hz, 1H), 7.88 (dd, *J* = 8.8, 1.8 Hz, 1H), 7.73–7.78 (m, 1H), 7.24–7.30 (m, 8H), 6.99 (dd, *J* = 7.4, 7.4 Hz, 8H), 6.84 (t, *J* = 7.4 Hz, 4H). ^{13}C NMR (d_6-DMSO): 162.6–164.1 (m), 156.7, 136.3, 135.5, 133.7, 130.8, 128.2, 125.3, 121.5, 47.8. HRESI-MS (pos.): 110.0608, calc. for **1**$^+$ $[C_6H_6NO]^+$ = 110.0606 Da. HRESI-MS (neg.): 319.1661, calc. for BPh_4^- $[C_{24}H_{20}B]^-$ = 319.1658 Da.

2·BPh$_4$: A solution of **2·I** (0.718 g, 2.50 mmol) in MeOH (25 mL) was added to a solution of $NaBPh_4$ (1.03 g, 3.00 mmol) in MeOH (25 mL) giving a pale yellow solution. After about 15 seconds, pale crystals began to form, and the reaction was left to stand at room temperature for an hour, and then in a freezer for an hour. After this time, the pale yellow crystals were isolated by filtration, washed with MeOH (3 × 5 mL), and thoroughly air-dried to give **2·BPh$_4$**. Yield: 1.04 g (2.17 mmol, 87%).

^{1}H NMR (d_6-DMSO): 9.16 (d, *J* = 5.7 Hz, 1H), 9.05 (d, *J* = 8.1 Hz, 1H), 7.95 (dd, *J* = 8.4, 8.4 Hz, 1H), 7.75–7.80 (m, 2H), 7.51–7.56 (m, 1H), 7.12–7.21 (m, 8H), 6.92 (dd, *J* = 7.4, 7.2 Hz, 8H), 6.78 (t, *J* = 7.2 Hz, 4H), 4.80 (s, 3H). ^{13}C NMR (d_6-DMSO) 162.8–164.2 (m), 151.2, 150.0, 147.1, 135.7, 132.0, 130.6, 129.5, 125.5, 121.73, 121.70, 120.7, 119.7, 51.5. HRESI-MS (pos.): 160.0764, calc. for **2**$^+$ $[C_{10}H_{10}NO]^+$ = 160.0762 Da. HRESI-MS (neg.): 319.1663, calc. for BPh_4^- $[C_{24}H_{20}B]^-$ = 319.1658 Da. ESI-MS (pos.): 639.3, calc. for $[\mathbf{2}_2{\cdot}BPh_4]^+$ *i.e.* $[C_{44}H_{40}BN_2O_2]^+$ = 639.3 Da.

2·Cl: A solution of **2·BPh$_4$** (0.240 g, 0.500 mmol) in acetone (10 mL) was added to a solution of TBA·Cl (0.167 g, 0.600 mmol) in acetone (10 mL) resulting in the immediate formation of a pale yellow precipitate. The suspension was swirled briefly, left to stand for 30 minutes and then the solid was isolated by filtration, washed with acetone (3 × 3 mL) and thoroughly air-dried to give **2·Cl** as a yellow powder. Yield: 0.096 g (0.049 mmol, 98%).

^{1}H NMR (d_6-DMSO): 12.20 (s, 1H), 9.30 (d, *J* = 5.6 Hz, 1H), 9.10 (d, *J* = 8.4 Hz, 1H), 8.00 (dd, *J* = 8.4, 5.7 Hz, 1H), 7.75–7.82 (m, 3H), 4.83 (s, 3H). ^{13}C NMR (d_6-DMSO): 151.1, 150.2, 146.9, 131.8, 130.3, 129.4, 121.5, 120.2, 119.7, 51.2. HRESI-MS (pos.): 160.0764, calc. for **2**$^+$ $[C_{10}H_{10}NO]^+$ = 160.0762 Da.

3·Br$_2$: 8-Hydroxyquinoline (2.90 g, 20.0 mmol) was dissolved in acetonitrile (50 mL) and the solution heated to reflux. Solid 1,2-bis(bromomethyl)benzene (0.528 g, 2.00 mmol) was added and the solution heated at reflux for 24 hours under a nitrogen atmosphere, during which time the colourless solution turned yellow and a yellow precipitate developed. The reaction was concentrated under reduced pressure and acetonitrile (20 mL) was added, the suspension was sonicated for 15 minutes, refluxed for 15 minutes and then cooled to room temperature. It was filtered, and the resulting yellow powder washed with acetonitrile (3 × 5 mL) and air-dried. Analysis by ^{1}H NMR spectroscopy indicated that the compound was approximately 90% pure at this point, and the yield at this point was 0.615 g (~ 55%, see Figure S7 for ^{1}H NMR spectrum of this material).

The crude product was dry-loaded onto silica (~ 10 mL) and added to the top of a column of silica (~ 25 mL) in 9:1 DCM:MeOH. Approximately 250 mL of 9:1 DCM:MeOH was eluted to remove an orange impurity, and then the eluent was switched to 88:10:2 DCM:MeOH:NEt_3, which caused the yellow compound at the top of the column to turn purple. The column was eluted with 200 mL of this solvent to remove a small purple band and then the eluent switched to 83:15:2 DCM:MeOH:NEt_3 (~ 250 mL) to remove a large purple band. This was concentrated *in vacuo* to give a purple solid. This was dissolved in 9:1 DCM:MeOH (20 mL) to give a deep purple solution, to which was added dropwise conc. $HBr_{(aq)}$. Addition of HBr initially caused a colour change from deep purple to bright red-orange and the development of a precipitate. Continued addition of $HBr_{(aq)}$ caused the colour to change to a bright yellow colour, at which point addition was stopped (0.3–0.4 mL $HBr_{(aq)}$ was added in total). The yellow suspension was left to stand for 30 minutes, and then filtered to give a lemon-yellow powder, which was washed with 9:1 DCM:MeOH (3 × 5 mL), DCM (3 × 5 mL), and then dried *in vacuo*. Yield of **3·Br$_2$**: 0.368 g (0.664 mmol, 33%).

^{1}H NMR (d_6-DMSO): 11.88 (br. s, 2H), 9.45 (d, *J* = 5.7 Hz, 2H), 9.23 (d, *J* = 8.3 Hz, 2H), 8.10–8.15 (m, 2H), 7.87 (d, *J* = 7.9 Hz, 2H), 7.79 (dd, *J* = 7.9, 7.9 Hz, 2H), 7.48 (d, *J* = 7.9 Hz, 2H), 7.13 (s, 4H), 6.56 (s, 4H). ^{13}C NMR (d_6-DMSO): 151.8, 148.8, 148.4, 136.4, 132.4, 130.7, 128.4, 126.7, 122.1, 121.2, 120.2, 63.6. HRESI-MS (pos.): 197.0840, calc. for **3**$^{2+}$ *i.e.* $[C_{26}H_{20}N_2O_2]^{2+}$ = 197.0835 Da. ESI-MS (pos.): 473.1, calc. for $[\mathbf{3}{\cdot}Br]^+$ *i.e.* $[C_{26}H_{22}N_2O_2Br]^+$ = 473.1 Da.

*This reaction to produce **3·Br$_2$** also produced **4·Br**, which we were able to isolate in small quantities (see Supporting Information).*

3·(PF$_6$)$_2$: A solution of **3·Br$_2$** (0.277 g, 0.500 mmol) in 3:1 H_2O:MeOH (30 mL) was added to a solution of NH_4PF_6 (0.196 g, 1.20 mmol) in H_2O (10 mL) containing 10 drops of 1% $HPF_{6(aq)}$ resulting in the immediate formation of a precipitate. The suspension was left to stand for 30 minutes and then filtered to give a very pale yellow powder, which was washed with water (3 × 5 mL), air-dried and then dried thoroughly *in vacuo* (< 10 mbar, 50 °C). Yield: 0.318 g (0.464 mmol, 93%).

^{1}H NMR (d_6-DMSO): 11.90 (br. s, 2H), 9.43 (d, *J* = 5.4 Hz, 2H), 9.22 (d, *J* = 8.0 Hz, 2H), 8.11–8.14 (m, 2H), 7.87 (d, *J* = 7.7 Hz, 2H), 7.79 (dd, *J* = 7.9, 7.9 Hz, 2H), 7.47 (d, *J* = 7.7 Hz, 2H), 7.13 (s, 4H), 6.55 (s, 4H). ^{13}C NMR (d_6-DMSO): 151.8, 149.0, 148.4, 136.5, 132.4, 130.7, 128.5, 126.7, 122.0, 121.1, 120.3, 63.7. ^{19}F NMR (d_6-DMSO): –70.2 (d, *J* = 711 Hz). ^{31}P NMR (d_6-DMSO): –144.2 (sept., *J* = 711 Hz). HRESI-MS (pos.): 197.0840, calc. for **3**$^{2+}$ *i.e.* $[C_{26}H_{20}N_2O_2]^{2+}$ = 197.0835 Da. ESI-MS (pos.): 931.4, calc. for $[\mathbf{3}^{-H}{}_2{\cdot}PF_6]^+$ *i.e.* $[C_{52}H_{42}N_4O_4F_6P]^+$ = 931.3 Da. ESI-MS (neg.): 145.0, calc. for PF_6^- = 145.0 Da.

3^{-H}·PF$_6$: **3·(PF$_6$)$_2$** (0.127 g, 0.200 mmol) was dissolved in MeOH (20 mL) with gentle heating. NEt_3 (28 □L, 20 mg, 0.20 mmol) was added to the hot yellow solution resulting in a change to a deep red colour. Within a few seconds, a bright orange precipitate developed. The suspension was cooled to room temperature

and then left to stand for 10 minutes. It was then filtered to isolate a bright orange precipitate, which was washed with MeOH (3 × 3 mL), Et_2O (3 × 3 mL), air-dried and then dried thoroughly *in vacuo*. Yield: 0.106 g (0.196 mmol, 98%).

^{1}H NMR (d_6-DMSO): 9.15 (d, *J* = 5.5 Hz, 2H), 8.97 (d, *J* = 8.3 Hz, 2H), 7.86–7.90 (m, 2H), 7.48 (dd, *J* = 7.9, 7.9 Hz, 2H), 7.30 (d. *J* = 7.6 Hz, 2H), 7.18 (s, 4H), 6.99 (d, *J* = 7.9 Hz, 2H). 6.80 (s, 4H). ^{13}C NMR (d_6-DMSO): 154.8, 149.5, 148.0, 136.9, 132.9, 131.1, 129.6, 127.3, 121.2, 120.9, 116.1, 62.6. ^{19}F NMR (d_6-DMSO): –70.2 (d, *J* = 711 Hz). ^{31}P NMR (d_6-DMSO): –144.2 (sept., *J* = 711 Hz). HRESI-MS (pos.): 393.1609, calc. for $\mathbf{3^{-H}}$ *i.e.* $[C_{26}H_{21}N_2O_2]^+$ = 393.1603 Da. ESI-MS (neg.): 144.8, calc. for PF_6^- = 145.0 Da.

Conflicts of interest

There are no conflicts to declare.

Acknowledgements

We thank the Australian Research Council for financial support (Australian Government Research Training Program Scholarships to RJG and MTB, FL170100041 to MLC, DE170100200 to NGW). MLC acknowledges generous allocations of supercomputing time on the National Facility of the Australian National Computational Infrastructure. We thank Dr Naomi Haworth for preliminary computational calculations, Dr Stephanie Boer for useful discussions, and Dr Michael Gardiner for assistance with synchrotron X-ray crystallography studies. Parts of this work were conducted using the MX1[60] and MX2[43] beamlines at the Australian Synchrotron.

Notes and references

1. N. H. Evans and P. D. Beer, *Angew. Chem., Int. Ed.*, 2014, **53**, 11716-11754.
2. L. Chen, S. N. Berry, X. Wu, E. N. W. Howe and P. A. Gale, *Chem*, 2020, **6**, 61-141.
3. J. Cai and J. L. Sessler, *Chem. Soc. Rev.*, 2014, **43**, 6198-6213.
4. T. M. Beale, M. G. Chudzinski, M. G. Sarwar and M. S. Taylor, *Chem. Soc. Rev.*, 2013, **42**, 1667-1680.
5. J. Y. C. Lim and P. D. Beer, *Chem*, 2018, **4**, 731-783.
6. S. A. Boer, E. M. Foyle, C. M. Thomas and N. G. White, *Chem. Soc. Rev.*, 2019, **48**, 2596-2614.
7. J. M. Coterón, F. Hacket and H.-J. Schneider, *J. Org. Chem.*, 1996, **61**, 1429-1435.
8. H. Miyaji and J. L. Sessler, *Angew. Chem., Int. Ed.*, 2001, **40**, 154-157.
9. K. J. Winstanley, A. M. Sayer and D. K. Smith, *Org. Biomol. Chem.*, 2006, **4**, 1760-1767.
10. J.-I. Kim, H. Juwarker, X. Liu, M. S. Lah and K.-S. Jeong, *Chem. Commun.*, 2010, **46**, 764-766.
11. M. J. Kim, H.-W. Lee, D. Moon and K.-S. Jeong, *Org. Lett.*, 2012, **14**, 5042-5045.
12. K. L. Wong, G. L. Law, Y. Y. Yang and W. T. Wong, *Adv. Mater.*, 2006, **18**, 1051-1054.
13. C. H. Chen and F. P. Gabbaï, *Angew. Chem. Int. Ed.* , 2018, **57**, 521-525.
14. N. Busschaert, C. Caltagirone, W. Van Rossom and P. A. Gale, *Chem. Rev.* , 2015, **115**, 8038-8155.
15. X. Wu, A. M. Gilchrist and P. A. Gale, *Chem*, 2020, **6**, 1296-1309.
16. N. G. White and M. J. MacLachlan, *Chem. Sci.*, 2015, **6**, 6245-6249.
17. C.-F. Ng, H.-F. Chow, D. Kuck and T. C. W. Mak, *Cryst. Growth Des.*, 2017, **17**, 2822-2827.
18. J. W. A. Harrell, M. L. Bergmeyer, P. Y. Zavalij and J. T. Davis, *Chem. Commun.*, 2010, **46**, 3950-3952.
19. X.-D. Wang, S. Li, Y.-F. Ao, Q.-Q. Wang, Z.-T. Huang and D.-X. Wang, *Org. Biomol. Chem.*, 2016, **14**, 330-334.
20. T. Saha, S. Dasari, D. Tewari, A. Prathap, K. M. Sureshan, A. K. Bera, A. Mukherjee and P. Talukdar, *J. Am. Chem. Soc.*, 2014, **136**, 14128-14135.
21. A. G. Schafer, J. M. Wieting, T. J. Fisher and A. E. Mattson, *Angew. Chem., Int. Ed.*, 2013, **52**, 11321-11324.
22. K. M. Engle, L. Pfeifer, G. W. Pidgeon, G. T. Giuffredi, A. L. Thompson, R. S. Paton, J. M. Brown and V. Gouverneur, *Chem. Sci.*, 2015, **6**, 5293-5302.
23. K. M. Diemoz, S. O. Wilson and A. K. Franz, *Chem. Eur. J.*, 2016, **22**, 18349-18353.
24. A. Shokri, J. Schmidt, X.-B. Wang and S. R. Kass, *J. Am. Chem. Soc.*, 2012, **134**, 16944-16947.
25. A. Shokri, X.-B. Wang and S. R. Kass, *J. Am. Chem. Soc.*, 2013, **135**, 9525-9530.
26. E. Faggi, R. Porcar, M. Bolte, S. V. Luis, E. García-Verdugo and I. Alfonso, *J. Org. Chem.*, 2014, **79**, 9141-9149.
27. M. Morshedi, S. A. Boer, M. Thomas and N. G. White, *Chem. Asian J.*, 2019, **14**, 1271-1277.
28. J. P. Saxena, W. H. Stafford and W. L. Stafford, *J. Chem. Soc.*, 1959, 1579-1587.
29. S. L. Shapiro, K. Weinberg and L. Freedman, *J. Am. Chem. Soc.*, 1959, **81**, 5140-5145.
30. In the case of the PF_6^- salts, the ^{19}F NMR spectrum was recorded in a solution containing a known amount of 2,2,2-trifluoroethanol. A delay time of 30 seconds was used between scans to ensure complete relaxation of the fluorine nuclei, see: a) W. He, F. Du, Y. Wu, Y. Wang, X. Liu, H. Liu and. X. Zhao, *J. Fluorine Chem.* 2006, **127**, 809-815; b) A. O. Mattes, D. Russell, E. Tishchenko, Y. Liu, R. H. Cichewicz and S. J. Robinson, *Concepts Magn. Reson.*, 2016, **45A**, e21422.
31. A peak for the O–H···O$^-$ hydrogen atom appears to be located halfway between the two oxygen atoms. In both structures, this is a special position, so the hydrogen atom was placed on this position, *i.e*. exactly halfway between the two oxygen atoms 1.21 Å from each atom.
32. A. L. Spek, *Acta Crystallogr.*, 2015, **C71**, 9-18.
33. S. F. Mason, *J. Chem. Soc.*, 1958, 674-685.
34. We acidified a solution of $\mathbf{3{\cdot}Br_2}$ with $HBr_{(aq)}$ and then titrated in $NaOH_{(aq)}$ while monitoring the pH of the solution using a pH meter. At a pH of approximately 5.5, a faint orange colour began to appear, consistent with deprotonation beginning to occur. By a pH of 6, precipitation occurred and so we were not able to measure further.
35. We were not possible to follow the O–H resonance in any of the anion binding studies reported herein. Even when no D_2O or MeOD was used in the solvent mixture, these peaks were not well-resolved. In the case of $\mathbf{1^+}$ in CD_3CN, we could not see this proton resonance at all. In the case

of **2**$^{+}$ in CD_3CN, it was visible but very broad and weak and thus not suitable for monitoring quantitative binding. Qualitatively, it showed a significant movement ~ 4 ppm, and a similar trend to that observed for C-H proton resonances.

36. *Bindfit*, accessed at supramolecular.org
37. Sulfate is not appreciably basic, and indeed the conjugate base of sulfate, HSO_4^-, appears to protonate **3**$^{-H+}$, the deprotonated form of **3**$^{2+}$ (Figure S28). As shown in Figure S25, addition of sulfate to **2**$^{+}$ in CH_3CN causes a purple colour (as opposed to the orange colour that results from deprotonation), but it is unclear what the cause of this is.
38. A. Albert and J. N. Phillips, *J. Chem. Soc.*, 1956, 1294-1304.
39. P. Thordarson, *Chem. Soc. Rev.*, 2011, **40**, 1305-1323.
40. S. Alvarez, *Dalton Trans.*, 2013, **42**, 8617-8636.
41. M. Szafran, A. Komasa, A. Katrusiak, Z. Dega-Szafran and P. Barczyński, *J. Mol. Struct.*, 2007, **844-845**, 102-114.
42. A structure of **2·Cl** as its hydrate has been reported. In this structure the O–H group of **2**$^{+}$ hydrogen bonds to a water molecule, which then hydrogen bonds to a Cl^- anion, *i.e*. there are no direct H-bonds from **2**$^{+}$ to the anion. C. Romming and E. Uggerud, *Acta Chem. Scand.* 1983, **37b**, 791-795.
43. D. Aragao, J. Aishima, H. Cherukuvada, R. Clarken, M. Clift, N. P. Cowieson, D. J. Ericsson, C. L. Gee, S. Macedo, N. Mudie, S. Panjikar, J. R. Price, A. Riboldi-Tunnicliffe, R. Rostan, R. Williamson and T. T. Caradoc-Davies, *J. Synchrotron Radiat.*, 2018, **25**, 885-891.
44. M. W. Hosseini, R. Ruppert, P. Schaeffer, A. De Cian, N. Kyritsakas and J. Fischer, *J. Chem. Soc., Chem. Commun.*, 1994, 2135-2136.
45. S. J. Brooks, P. A. Gale and M. E. Light, *CrystEngComm*, 2005, **7**, 586-591.
46. N. G. White and M. J. MacLachlan, *Cryst. Growth Des.*, 2015, **15**, 5629-5636.
47. X. He, S. Hu, K. Liu, Y. Guo, J. Xu and S. Shao, *Org. Lett.*, 2006, **8**, 333-336.
48. Measurement of the anion recognition properties of the protonated form of DBU, the base we used to measure pK_as in an organic solvent show it interacts relatively weakly with chloride (K_a = 419 M^{-1}). Hence we expected the stronger interaction of Cl^- with **2**$^{+}$ over DBU^{H+} to favour the protonated form of the O–H receptor. See Supporting Information for further details, and synthesis and X-ray crystal structure of $DBU^{H}\cdot PF_6$.
49. The shortest C–H···halide hydrogen bond observed is 96% of Σ_{vdW} in the structure of **3·Br$_2$** (whereas O–H···halide hydrogen bond distances range from 71-80% of Σ_{vdW}). Slightly shorter C–H···sulfate hydrogen bonds are seen in the structures of **2$_2$·SO$_4$** and **3·SO$_4$** (88 and 89% Σ_{vdW}), although these are significantly longer than the O–H···sulfate hydrogen bonds (64-66% Σ_{vdW}).
50. Y. Zhao and D. G. Truhlar, *Theor. Chem. Acc.*, 2008, **120**, 215-241.
51. A. V. Marenich, C. J. Cramer and D. G. Truhlar, *J. Phys. Chem. B*, 2009, **113**, 6378-6396.
52. M. M. Fickling, A. Fischer, B. R. Mann, J. Packer and J. Vaughan, *J. Am. Chem. Soc.*, 1959, **81**, 4226-4230.
53. D. K. Smith, *Org. Biomol. Chem.*, 2003, **1**, 3874-3877.
54. R. Pizer and L. Babcock, *Inorg. Chem.*, 1977, **16**, 1677-1681.
55. We note that while the halide binding properties are similar, these receptors display signifcantly stronger sulfate binding than **1**$^{+}$. See Ref 28.
56. C. J. Serpell, A. Y. Park, C. V. Robinson and P. D. Beer, *Chem. Commun.*, 2021, **57**, 101-104.
57. W. W. H. Wong, M. S. Vickers, A. R. Cowley, R. L. Paul and P. D. Beer, *Org. Biomol. Chem.*, 2005, **3**, 4201-4208.
58. Y. Mao, M. Loipersberger, K. J. Kron, J. S. Derrick, C. J. Chang, S. M. Sharada and M. Head-Gordon, *Chem. Sci.*, 2021, **12**, 1398-1414.
59. R. A. Lowe, D. Taylor, K. Chibale, A. Nelson and S. P. Marsden, *Bioorg. Med. Chem.*, 2020, **28**, 115442.
60. N. P. Cowieson, D. Aragao, M. Clift, D. J. Ericsson, C. Gee, S. J. Harrop, N. Mudie, S. Panjikar, J. R. Price, A. Riboldi-Tunnicliffe, R. Williamson and T. Caradoc-Davies, *J. Synchrotron Radiat.*, 2015, **22**, 187-190.